CHAPTER 14

BULK-MODULI SYSTEMATICS IN OXIDES, INCLUDING SUPERCONDUCTORS

Hassel Ledbetter and Sudook Kim
Materials Science and Engineering Laboratory, National Institute of Standards and Technology, Boulder, Colorado, USA

Contents

ABSTRACT

For oxides, including superconductors, we consider the systematics of the bulk-modulus/atomic-volume (B/V_a) relationship. For nonsuperconducting oxides, the B–V_a diagram shows that most oxides fall in three sets: (1) rocksalt crystal structure, AO; (2) perovskite crystal structure, ACO_3; and (3) transition-metal oxides ranging through stoichiometries of AO, A_3O_4, A_2O. Seventeen oxide superconductors show a surprisingly narrow V_a range and a relatively narrow range of $B = 116 \pm 19$ GPa. B–V_a slopes depart from expectations from a simple ionic-crystal model. Within a superconductor subgroup, for example, La–O or T1–O, higher B corresponds to higher T_c. Because the in-plane (CuO_2-plane) compressibility probably varies little among these cuprates, the out-of-plane compressibility should correlate inversely with T_c.

14.1. INTRODUCTION

The bulk modulus B, or reciprocal compressibility, represents a solid's most basic elastic constant. It shows a material's resistance to interatomic-distance changes caused by hydrostatic pressure. Bulk modulus, atomic volume, and cohesive energy comprise

the three fundamental cohesive properties, which relate, in turn, to many other solid-state physical properties.

For superconductors, the bulk modulus enters in two further ways. First, it helps determine the Debye characteristic temperature θ_D, which enters the preexponential factor in the BCS equation for critical temperature for phonon-mediated electron-pair superconductivity [1]:

$$T_c = 1.14\theta_d \exp(-1/\lambda) \tag{14.1}$$

Second, McMillan [2] showed that the electron–phonon parameter λ depends on θ_D, thus on B.

For oxide superconductors, the present study focuses on the B–V_a relationship, where V_a denotes mean atomic volume, the unit-cell volume divided by the number of atoms per unit cell. We consider the superconductors against the background of nonsuperconducting oxides, especially perovskite and rocksalt crystal structures, which form crystal-structure building blocks for most of the superconductors.

14.2. SOURCES

For $SrTiO_3$ and $BaTiO_3$, we measured B on monocrystals by ultrasonic methods [3]. For $BaBiO_3$, we used a theoretical result [4]. For all other nonsuperconducting oxides, we used published usual-source acoustic values from measurements on monocrystals. For the 17 superconductors, we used 9 neutron-diffraction results summarized by Izumi [5]. Reliable acoustic bulk moduli are available for only a few superconductors because existing monocrystals are too small for usual measurement methods, and polycrystals contain voids or microcracks, which blur the intrinsic bulk-modulus value. However, to fill out the study we used four of our polycrystal La–O results [6], which seem not to suffer from the crack-void problem, where apparent elastic stiffness is always lower than intrinsic. For four compounds, we calculated B from the crystal structure and assumed valences by using a rigid-ion ionic-crystal model [7]. These four compounds were $La_{1.85}Sr_{1.15}Cu_2O_6$, $Tl_2Ba_2Ca_2Cu_3O_{10}$, $Bi_2Sr_2CuO_6$, and $Bi_2Sr_2Ca_2Cu_3O_{10}$. For all 17 superconductors, Table 14.1 shows the B and V_a values.

Table 14.1. Oxide superconductor properties.

	V_a $(\mathring{A}^3)$	B (GPa)	Source
$La_{1.85}Sr_{0.15}CuO_4$	13.50	147.0	Izumi [5]
$Nd_{1.32}Sr_{0.41}Ce_{0.27}CuO_4$	13.26	143.0	Izumi [5]
$Nd_{1.835}Ce_{0.165}CuO_4$	13.44	140.0	Izumi [5]
Nd_2CuO_4	13.50	134.0	Izumi [5]
$La_{1.82}Ca_{1.18}Cu_2O_6$	12.89	133.0	Izumi [5]
$YBa_2Cu_3O_{6.93}$	13.41	123.0	Izumi [5]
La_2CuO_4	13.61	122.0	NIST, meas.
$YBa_2Cu_4O_8$	13.50	117.8	Izumi [5]
Pr_2CuO_4	13.65	115.3	NIST, meas.
$YBa_2Cu_3O_{6.6}$	14.65	112.0	Izumi [5]
$La_{1.85}Sr_{1.15}Cu_2O_6$	13.49	109.3	NIST, calc.
$Tl_2Ba_2Ca_2Cu_3O_{10}$	13.92	108.1	NIST, calc.
$La_{1.85}Ba_{0.15}CuO_4$	13.51	107.6	NIST, meas.
$Bi_2Sr_2Ca_2Cu_3O_{10}$	14.10	95.95	NIST, calc.
$La_{1.85}Ca_{0.15}CuO_4$	13.46	90.28	NIST, meas.
$Bi_2Sr_2CuO_6$	16.13	89.84	NIST, calc.
$Tl_2Ba_2CuO_6$	15.77	82.64	Izumi [5]
Mean:	13.87 ± 0.87	115.9 ± 19.4	

For V_a values, we used either results summarized by Hazen [8] or original-literature values. Here, we omit these references because, for our purposes, V_a varies little among various reports.

14.3. RESULTS

Figure 14.1 shows results for nonsuperconducting oxides. Three trend lines appear: perovskite structure, rocksalt structure, and transition-metal-cation compounds. We consider the slopes in the following way:

$$B \sim V_a^{-n/3} \sim d^{-n} \tag{14.2}$$

Here d denotes a characteristic interatomic distance. From Figure 14.1, we find $n = 2.35$ (perovskite), $n = 2.82$ (rocksalt), and $n = 5.74$ (transition-metal-cation).

Against these three trend lines, Figure 14.2 shows results for 17 oxide superconductors.

14.4. DISCUSSION

We expect the perovskite line to lie above the rocksalt line because the M^{4+} cation increases the Madelung energy, and thus increases the cohesive energy and bulk modulus [9]. Also, the perovskite compounds may contain more covalent bonding than the rocksalt compounds.

The trend-line slopes present some surprises. From a simple B or n pure-ionic-bond model, we expect $B \sim d^{-4}$, that is $n = 4$ [9]. The rocksalt case, $n \simeq 3$, suggests that these materials fail to fit such a simple ionic model. The perovskite case, $n \simeq 2.5$, may reflect covalent bonding or the complication of d-shell-electron cations. Certainly, this latter complication appears in the third trend line for oxides containing only transition-metal cations. The strong slope, $n \simeq 6$, about double the perovskite and rocksalt slopes, agrees with the fact that transition elements in a given periodic-table row show similar
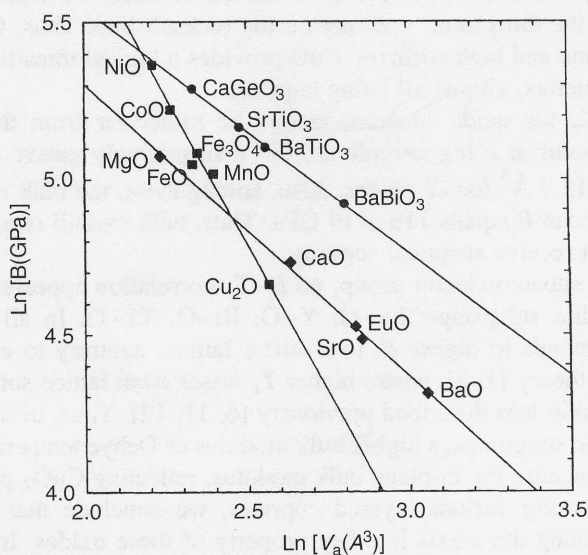

Fig. 14.1. Log–log diagram of bulk modulus versus mean atomic volume for various oxides. Three trend lines emerge: perovskite structure, rocksalt structure, and compounds containing transition-metal cations.
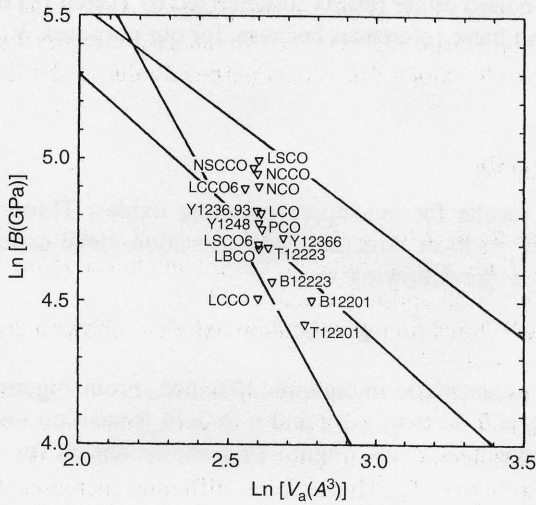
Fig. 14.2. Same diagram as Figure 14.1, but for oxide superconductors. We see a very limited range of V_a and a fairly limited range of B. For 17 cases, V_a (mean) $= 13.9 \pm 0.9 \ Å^3$ and B (mean) $= 116 \pm 19$ GPa. For comparison purposes, the trend lines established in Figure 14.1 are transferred to Figure 14.2.

Key:

LSCO = $La_{1.85}Sr_{0.15}CuO_4$

NCCO = $Nd_{1.835}Ce_{0.165}CuO_4$

NCO = Nd_2CuO_4

LCO = La_2CuO_4

LBCO = $La_{1.85}Ba_{0.15}CuO_4$

Y1248 = $YBa_2Cu_4O_8$

PCO = Pr_2CuO_4

Y1236.93 = $YBa_2Cu_3O_{6.93}$

LCCO6 = $La_{1.82}Ca_{1.18}Cu_2O_6$

NSCCO = $Nd_{1.32}Sr_{0.41}Ce_{0.27}CuO_4$

Y12366 = $YBa_2Cu_3O_{6.6}$

LSCO6 = $La_{1.85}Sr_{1.15}Cu_2O_6$

Tl2223 = $Tl_2Ba_2Ca_2Cu_3O_{10}$

Bl2223 = $Bl_2Sr_2Ca_2Cu_3O_{10}$

LCCO = $La_{1.85}Ca_{0.15}CuO_4$

Bl2201 = $Bl_2Sr_2CuO_6$

TL2201 = $Tl_2Ba_2CuO_6$

atomic volumes but strongly different properties [10]. This third trend line also emphasizes that copper behaves as a transition element, that its 3d-electrons enter bonding, that the usual $3d^{10}4s^1$ electron structure is too naive. Thus, we would expect CuO to lie near NiO on the third trend line, not on the rocksalt line. Thus, CuO would show low atomic volume and high stiffness. CuO provides a logical transition to the high-T_c oxide superconductors, almost all being cuprates.

In Figure 14.2, the oxide superconductors lie rather far from the expected CuO position. They occur at a higher volume, but a surprisingly nearly constant volume: The mean $V_a = 13.9 \ Å^3$ for 17 oxides. Also, among these, the bulk-modulus variation is not so large: mean B equals 116 ± 19 GPa. Thus, bulk moduli reported well outside this range should receive skeptical scrutiny.

For the entire superconductor group, no $B-T_c$ correlation appears; however, correlations exist within subgroups: La–O, Y–O, Bi–O, Tl–O. In all subgroup cases, higher T_c corresponds to higher B, to a stiffer lattice, contrary to expectations from BCS–McMillan theory [1, 2], where higher T_c arises from lattice softening. A similar $T_c - \theta_D$ relationship was described previously [6, 11, 12]. Thus, in these oxide superconductors, within subgroups, a higher bulk modulus or Debye temperature corresponds to a higher T_c. Because the in-plane bulk modulus, reflecting CuO_2 planes, is presumably the same among various layered cuprates, we conclude that the out-of-plane compressibility along the c-axis is a key property of these oxides. In terms of elastic constants, this means a higher value, in orthorhombic symmetry, of the c-axis reciprocal linear compressibility [13]:

$$k_z^{-1} = (S_{13} + S_{23} + S_{33})^{-1} \tag{14.3}$$

Here, the S_{ij} denote the usual Voigt elastic compliances. Very roughly, this corresponds to maximizing the Voigt elastic stiffness C_{33}. On an atomic scale, this means increasing interatomic-bond strengths along the c-axis, perpendicular to the CuO_2 planes.

14.5. CONCLUSIONS

1. Perovskite oxides tend to be stiffer than rocksalt oxides.
2. In both cases, B decreases with increasing volume according to $B \sim d^{-n}$, where $n(\text{perovskite}) = 2.35$ and $n(\text{rocksalt}) = 2.82$.
3. The third case — transition-metal-cation oxides — shows a dramatically different $B-d$ behavior: $n = 5.74$.
4. A set of 17 oxide superconductors shows a surprisingly tight cluster on the $B-V_a$ diagram: B varying $\pm 16\%$, V_a varying $\pm 6\%$.
5. Within superconductor subgroups — La–O, Y–O, Bi–O, Tl–O — higher B corresponds to higher T_c. Thus, lattice stiffening increases T_c.
6. We should consider further the $T_c-k_z^{-1}$ relationship, where k_z denotes elastic linear compressibility along the c-axis.

References

1. Bardeen, J., Cooper, L., and Schrieffer, J. (1957). *Phys. Rev.* **108**: 1175, equation (3.29).
2. McMillan, W. (1968). *Phys. Rev.* **167**: 331.
3. Ledbetter, H., Frederick, N., and Austin, M. (1980). *J. Appl. Phys.* **51**: 305.
4. Liechtenstein, A., Mazin, I., Rodriquez, C., Jepsen, O., Andersen, O., and Methfessel, M. (1991). *Phys. Rev. B* **44**: 5388.
5. Izumi, F. (May 1993). In *Proceedings, ACA meeting, Albuquerque*, New Mexico: forthcoming.
6. Ledbetter, H., Kim, S., and Roshko, A. (1992). *Z. Phys. B-Cond. Matter* **89**: 129.
7. Ledbetter, H., and Lei, M. (1990). *Physica* **C166**: 483.
8. Hazen, R. (1990). In *Physical Properties of High Temperature Superconductors II*, pp. 121–198. Singapore: World Scientific.
9. Brown, F. (1967). *The Physics of Solids*, pp. 101–106. New York: Benjamin.
10. Moruzzi, V., Janak, J., and Williams, A. (1978). Calculated Electronic Properties of Metals, especially chapter 3. New York: Pergamon.
11. Ledbetter, H., Kim, S., and Roshko, A. (1991) *Physica* **C190**: 129.
12. Dominec, J. (1992). *Phys. Status Solidi (B)* **169**: K83.
13. Nye, J. (1960). Physical Properties of Crystals, p. 146. London: Oxford.